

Bright Heralded Source Reaching Theoretical Single-Photon Purity

Haoyang Wang,^{1, 2,*} Huihong Yuan,^{1,*} Qiang Zeng,^{1, †} Lai Zhou,¹ Haiqiang Ma,² and Zhiliang Yuan¹

¹*Beijing Academy of Quantum Information Sciences, Beijing 100193, China*

²*School of Science and State Key Laboratory of Information Photonics and Optical Communications, Beijing University of Posts and Telecommunications, Beijing 100876, China*

(Dated: June 13, 2024)

We derive the theoretical limit of single-photon purity of heralded single-photon sources, and accordingly demonstrate a bright, gigahertz-pulsed heralded source with the purity saturating the limit. Based on spontaneous four-wave mixing in a silicon spiral waveguide, this on-chip source is measured to have a coincidence rate exceeding 1.5 MHz at a coincidence to accidental (CAR) ratio of 16.77. The single-photon purity, quantified by the auto-correlation function $g_h^{(2)}(0)$, reaches the theoretical limit with the lowest value of 0.00094 ± 0.00002 obtained at a coincidence rate of 0.8 kHz. We attribute our results to effective spectral filtering as well as the coherent pump condition helped by optical injection locking.

I. INTRODUCTION

Single photon is a precious resource for quantum information applications [1]. They can be either produced on-demand by quantum emitters [2], or heralded from spontaneous parametric photon-pair generation processes [3, 4]. The latter approach has the advantage of room-temperature operation and inherent compatibility with photonic waveguide integration [5]. Particularly, achieving phase matching for spontaneous four-wave mixing (SFWM)—a third-order ($\chi^{(3)}$) nonlinear process—is relatively easy. To date, a broad class of on-chip SFWM sources has been developed on various material platforms [6], among which silicon-on-insulator (SOI) attracts a great deal of interest thanks to its compatibility with mature CMOS manufacturing technology.

Single-photon purity is a key parameter for evaluating the performance of an HSPS. It is measurable by the heralded auto-correlation function $g_h^{(2)}(0)$ using the setup shown in Fig. 1(a). While a value close to 0 is desirable for quantum applications, the actual $g_h^{(2)}(0)$ value of an HSPS depends on the source brightness. A stronger pump produces a higher number of heralded single photons per unit time, but at the intrinsic expense of single-photon purity due to the increased probability of multi-pairs. To complicate further, single-photon purity is strongly affected also by the residual pump or spontaneous Raman photons leaked into the heralded path through imperfect spectral filtering. So far, there lacks a simple criteria to determine whether an HSPS has reached its theoretical single-photon purity.

To bridge this gap, we derive an explicit theoretical limit for single-photon purity of HSPS sources under coherent pump condition. This limit is subsequently verified on a pulsed SFWM source, pumped by 2.5 GHz, 70 ps stable pulses that are seeded by a pair of laser

diodes in an optical injection locking configuration [7, 8]. The non-linear SFWM medium is a small-footprint spiral waveguide structure fabricated on SOI platform. Our source is characterized to have brightness-limited single-photon purity for the pump power varying over two orders of magnitude. Under a strong pump, it achieves an unprecedentedly high coincidence rate of 1.51 MHz with a coincidence-to-accidental ratio (CAR) of 16.77. The source under a weak pump is measured to have the lowest $g_h^{(2)}(0)$ value of 0.00094 ± 0.00002 together with a coincidence rate of 0.8 kHz.

II. THEORETICAL LIMIT OF $g_h^{(2)}(0)$

Figure 1 (a) depicts the schematic for a heralded Hanbury-Twiss Brown (HBT) setup for measuring the single-photon purity of an HSPS. A non-linear medium, either $\chi^{(2)}$ or $\chi^{(3)}$ material, is optically pumped to produce on average μ pairs of signal (s) and idler (i) photons per pump pulse when under pulsed excitation. In the case of a continuous wave pump, μ denotes the average number of generated photon pairs per temporal bin adopted in the measurement. Signal and idler photons are spatially separated. Detecting a photon at one path heralds another photon in the other path. Single-photon purity of an HSPS can then be characterized by the heralded auto-correlation function [5]

$$g_h^{(2)}(0) = \frac{\langle \hat{a}_1^\dagger \hat{a}_2^\dagger \hat{a}_3^\dagger \hat{a}_3 \hat{a}_2 \hat{a}_1 \rangle}{\langle \hat{a}_1^\dagger \hat{a}_2^\dagger \hat{a}_2 \hat{a}_1 \rangle \langle \hat{a}_1^\dagger \hat{a}_3^\dagger \hat{a}_3 \hat{a}_1 \rangle} \langle \hat{a}_1^\dagger \hat{a}_1 \rangle, \quad (1)$$

where a_j and a_j^\dagger ($j = 1, 2, 3$) are respectively photon annihilation and creation operators at port j .

A coherent pump produces Poissonian photon number distribution $P(n) = e^{-\mu} \frac{\mu^n}{n!}$ for signal and idler photons [9]. From this, $g_h^{(2)}(0)$ can be derived to have an explicit dependence on the mean photon-pair number μ

$$g_h^{(2)}(0) = 1 - \frac{1}{(\mu + 1)^2}. \quad (2)$$

* These authors contributed equally to this work.

† zengqiang@baqis.ac.cn

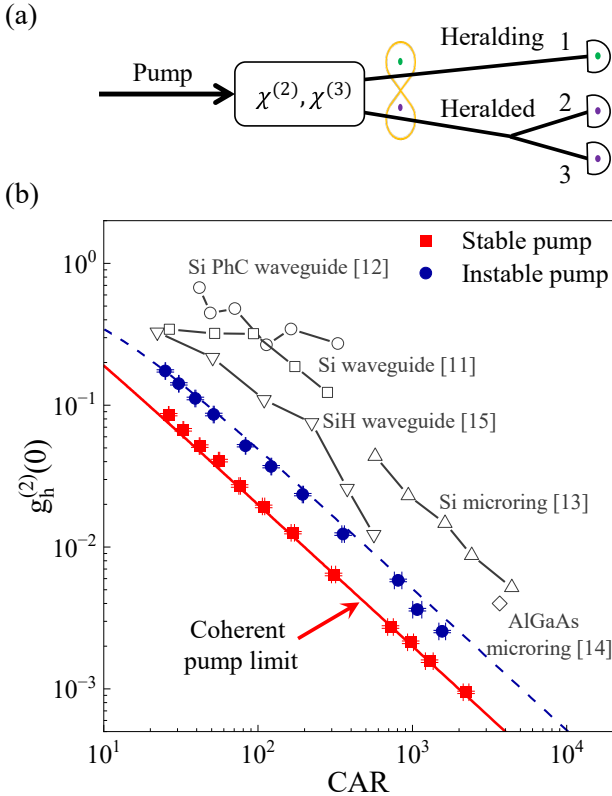


FIG. 1. (a) A schematic for measuring single-photon purity of HSPS. (b) $g_h^{(2)}(0)$ values, achieved in this work (solid symbols) or extracted from literature (open symbols). The red solid line denotes the theoretical limit under coherent pump condition, while the dashed line simulates an SFWM source under a pump with intensity fluctuation.

With this equation, one needs both the single-photon purity ($g_h^{(2)}(0)$) and the source brightness (μ) in order to identify the performance gap of an HSPS from its theoretical limit. However, μ is hard to be measured precisely, due to inevitable photon losses and noise photons.

CAR quantifies the temporal coherence of generated signal and idler photons, and is directly measurable using a cross-correlation setup [5]. In the absence of noise photons, CAR can be theoretically derived for a coherent pump as [10]

$$\text{CAR} = \frac{\langle \hat{a}_s^\dagger \hat{a}_i^\dagger \hat{a}_i \hat{a}_s \rangle}{\langle \hat{a}_s^\dagger \hat{a}_s \rangle \langle \hat{a}_i^\dagger \hat{a}_i \rangle} = 1 + \frac{1}{\mu}, \quad (3)$$

where $a_{s(i)}$ and $a_{s(i)}^\dagger$ are respectively annihilation and creation operators of signal and idler photons. Combining Eqs. (2) and (3), we obtain the theoretical limit for single-photon purity achievable with a coherent pump

$$g_h^{(2)}(0) = \frac{2\text{CAR} - 1}{\text{CAR}^2}. \quad (4)$$

This limit applies to all HSPS's under a coherent pump, including SPDC and SWFM sources. Since both param-

eters in Eq. (4) are directly measurable, the equation can be used to examine whether an HSPS has reached its potential for single-photon purity.

We compare in Fig. 1(b) the data (empty symbols) extracted from reported HSPS sources [11–15] to this theoretical limit (red line). None of the sources have reached the theoretical limit, even when CAR values exceeding 10^3 were obtained. Deviation from this limit can be caused by a number of factors, including detector dark counts, noise photons and/or intensity fluctuation in the pump. Detailed derivation for Eq. (2) is provided in Appendix A.

III. EXPERIMENTAL SETUP

Figure 2 shows our experimental setup. A pair of semiconductor distributed feedback (DFB) laser diodes both emitting at a wavelength of 1550.52 nm are used in an optical injection locking configuration [7] to generate seed pulses for amplification. Optical injection locking reduces time jitter and improves intensity stability of the SL gain-switched pulses [16]. While the master laser (ML) runs in continuous-wave mode, the slave laser (SL) is biased by a 2.5 GHz square waves to gain-switch around its threshold such that it produces 2.5 GHz, 70 ps laser pulses [8] of stable intensities. Switching off the ML allows us to purposely introduce strong intensity fluctuation to the pump pulses and thus demonstrate its effect on single-photon purity.

The seed pulses are amplified by an erbium-doped fiber amplifier (EDFA), followed by a fiber Bragg grating (FBG) with 0.4 nm (full width at half-maximum, FWHM) passband and a tunable bandpass filter (BPF) with 0.3 nm passband for removing residual pump photons with ≥ 106 dB isolation. The pump power is monitored by an optical power meter (PM) through a 10:90 tap beam splitter and then stabilized using a variable optical attenuator (VOA). The pump pulses are aligned by a polarization controller (PC) to TE mode of the silicon spiral waveguide.

In the spiral waveguide, two pump photons annihilate for creation of two daughter photons of frequencies ω_s (signal) and ω_i (idler), which symmetrically surround the pump frequency ω_p . To reject the residual pump, a dense wavelength divisional multiplexer (DWDM) which has 0.6 nm passbands and non-adjacent channel isolation no less than 105.5 dB, is applied after the spiral waveguide chip and we choose to use ITU channels C39 (1546.92 nm) and C28 (1554.94 nm) for the signal and idler outputs, respectively. The filtered photons are sent to a pair of superconducting nanowire single-photon detectors (SNSPDs) with their polarization controlled by a PC before each detector input for optimal detection efficiencies. To measure the heralded single-photon purity, one of the SNSPDs is replaced by the HBT setup (dashed box). These detectors feature about 71% detection efficiency, ~ 300 Hz dark count rate per channel, and 80 ps

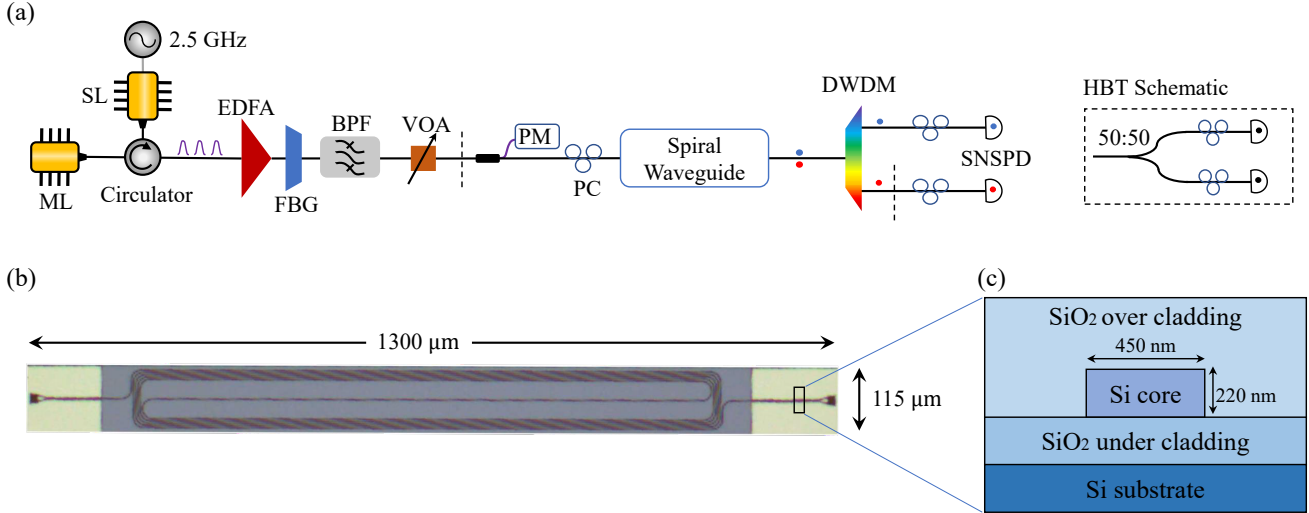


FIG. 2. (a) Experimental setup. The HBT setup (dashed box) is used to characterize the intensity fluctuation of the pump or to measure the single-photon purity, by placing it into locations as dashed lines show. ML: master laser, SL: slave laser, EDFA: erbium-doped fiber amplifier, FBG: fiber Bragg grating, BPF: band-pass filter, VOA: variable optical attenuator, PM: power meter, PC: polarization controller, DWDM: dense wavelength division multiplexer, SNSPD: Superconducting nanowire single photon detector. (b) Image of the rectangular spiral waveguide. (c) Schematic of waveguide cross-section.

time jitter. A multi-channel time-correlated single photon counting (TCSPC) instrument is used for correlation measurement.

We present the design of our SOI chip in Fig. 2(b) and (c). Fabricated on a Si wafer, the spiral waveguide is designed for TE mode transmission and has a cross-section dimension of $450 \times 220 \text{ nm}^2$. Each waveguide bend was designed to be no less than $22 \mu\text{m}$ in order to minimize losses. Additionally, an annealing process during fabrication was performed to reduce the waveguide sidewall roughness after dry etching the Silicon layer. The total length of the waveguide is about 1.3 cm, with a transmission loss of 2.6 dB/cm. Grating couplers are used to couple light between fiber and waveguide with a loss of around 4.5 dB per facet.

IV. RESULTS

We first characterize the auto-correlation of the pump signal using the HBT setup to ensure it obeys Poissonian photon number statistics. We start with the ML switched off and gain-switch the SL to output optical pulses at 2.5 GHz but with considerable intensity fluctuation. As revealed in Fig. 3(a), the corresponding auto-correlation function is bunched at 0-delay, which is a typical behavior for gain-switched lasers at near-threshold operation [18]. Noticeable coincidence dips at ± 0.4 ns delays imply negative correlation between adjacent laser pulses, as previously reported [19]. Turning on the ML and injecting 55 μW light, the SL output becomes stable in intensity as evidenced by the auto-correlation shown in Fig. 3(b). We obtain $g^{(2)}(0) = 1.010 \pm 0.004$, approaching the expected value of $g^{(2)}(0) = 1$ for a coherent light source. With a

small deviation, we consider the pump source as coherent and obeys Poissonian photon number distribution.

Under the coherent pump condition, we measure the single (S) and coincidence (C) counting rates as a function of the average pump power (P) entering the silicon spiral waveguide, i.e., the optical power after the fiber-to-chip coupling. As shown in Fig. 4(a), both the signal and idler counting rates show quadratic dependence on the pump power, which can be fit using [6]

$$S = aP^2 + bP + c, \quad (5)$$

where aP^2 , bP , and c represent the counting rates arising from SFWM photons, noise photons and detector dark counts, respectively. Coefficients a , b and c have the dimensions of $\text{MHz} \cdot \text{mW}^{-2}$, $\text{MHz} \cdot \text{mW}^{-1}$, and MHz , respectively. To avoid heralding efficiency saturation [20], we limit the fitting region to $\leq 3.00 \text{ mW}$ on-chip power and the fitted results are shown as solid lines. According to the fitting coefficients, the noise photon, i.e., the linear term bP dominates at very low pump powers, e.g., $P \leq 0.1 \text{ mW}$. These noise photons may arise from the residual pump and Raman photons leaked into the signal or idler channel. Note that the signal and idler channels do not have equal counting rates, which we attribute to the difference in the channel losses. For example, C28 and C39 channels of the DWDM have 1.23 dB and 0.68 dB losses, respectively. This inequality leads to asymmetric heralding efficiencies between C28 and C39 channels, as reported in Appendix B.

Figure 4 (b) shows the measured coincidence rates, together with a polynomial fitting. At a pump power of 7.10 mW, we obtain a coincidence rate of 1.51 MHz and a corresponding CAR of 16.77 ± 0.01 . To our knowledge,

TABLE I. State-of-the-art SFWM photon pair sources under pulsed excitation.

Ref	Material	Repetition rate	Max CAR	Min $g_h^{(2)}(0)$	Coincidence counts (CAR)
this work	Si waveguide	2.5 GHz	4630	0.00094 ± 0.00002	1.5 MHz (16.77)
[17]	Si waveguide	500 MHz	8	-	300 kHz (8)
[15]	Heterogeneous waveguide	50 MHz	1632.6	0.0126 ± 0.005	-
[12]	Si PhC waveguide	50 MHz	329	< 0.1	48 Hz (41)

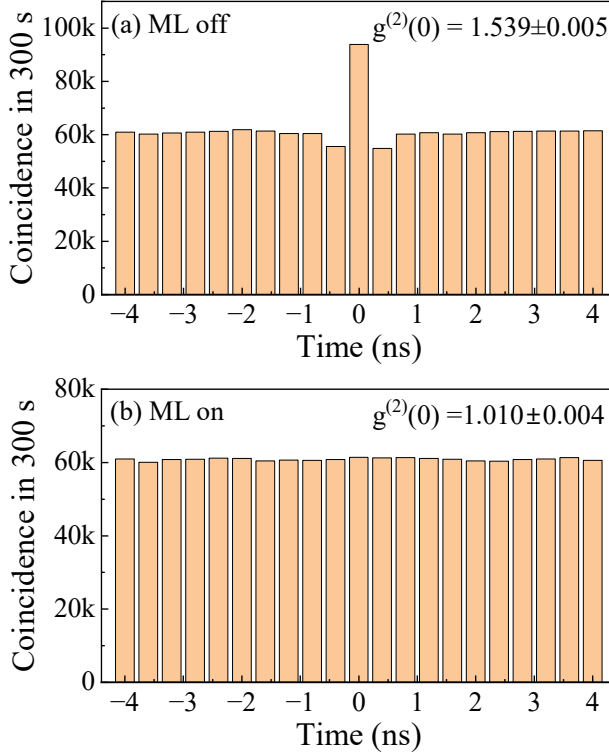
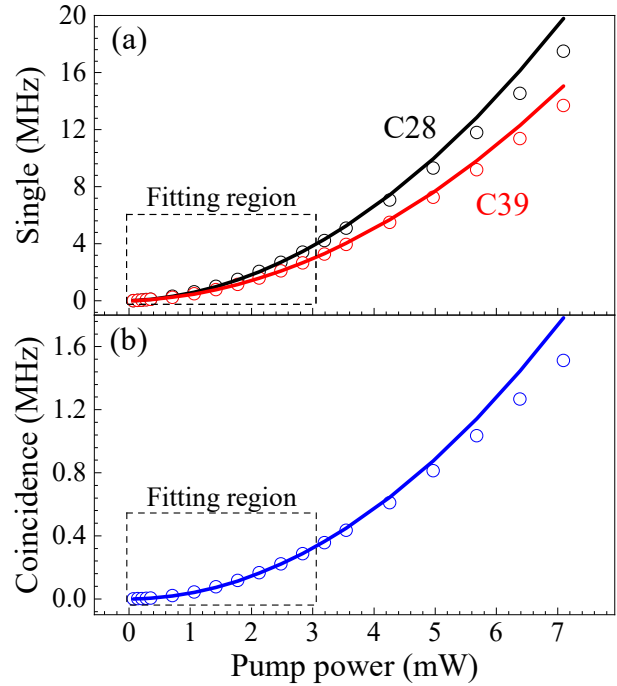


FIG. 3. Auto-correlations of the pump source under operational conditions. (a) master laser off, (b) master laser on.

the coincidence rate surpasses all previous results. Near-MHz coincidence rate was only achieved with an SPDC source but at a lower CAR of 7.5 [21]. In Fig. 5, we plot the measured CAR as a function of coincidence count rate. As expected from Eq. (3), the CAR value increases inversely with a decreasing coincidence rate C , with the highest CAR being 4630 ± 614 . We can simulate CAR using

$$\text{CAR} = \frac{C \cdot R}{S_s \cdot S_i} + 1, \quad (6)$$

where R is the repetition rate of the pump pulses and we use the polynomial fitting parameters obtained in Fig. 4 to calculate the single counting rates S_s and S_i of signal and idler photons. The simulation (solid line) reproduces excellently the dependence of CAR on the coincidence rate using just parameters extracted from experiments.

FIG. 4. Experimental results (symbols) and polynomial fittings (lines) for (a) single and (b) coincidence counting rates between DWDM channels C28 and C39. The polynomial fitting formulas are $S_s = 0.369P^2 + 0.171P + 0.0003$, $S_i = 0.278P^2 + 0.150P + 0.0003$ and $C = 0.032P^2 + 0.002P$ for single counting rate of signal (idler) photons and coincidence counting rate.

For more details and analysis on heralding efficiency and CAR, refer to Appendices B and C.

In order to compare against the theoretical limit for single-photon purity (Eq. (4)), we measure $g_h^{(2)}(0)$ and plot the measurement result together with error bars (red symbols) in Fig. 1. The lowest $g_h^{(2)}(0)$ was measured as 0.00094 ± 0.00002 , which is among the best $g_h^{(2)}(0)$ values reported to date for an HSPS. For overall $g_h^{(2)}(0)$ vs. CAR relation, the experimental data reach the theoretical limit, suggesting that our source produces the ideal single-photon purity permitted by a heralded source. We attribute this achievement to both effective spectral filtering in our setup and the coherent pump condition al-

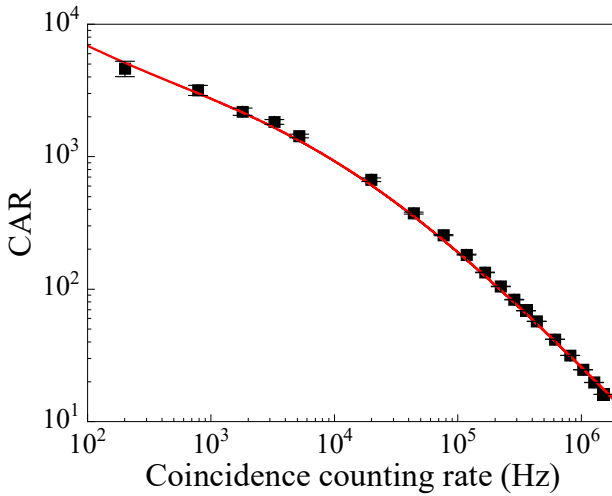


FIG. 5. CAR versus coincidence counting rate: measured results (symbols) and simulation (line).

lowed by optical injection locking.

Deviation from coherent pump condition will deteriorate the single-photon purity for a given CAR value. To demonstrate, we switch off the ML to introduce intensity fluctuation, leading to the pump to have a measured $g^{(2)}(0) = 1.539 \pm 0.005$ (see Fig. 3(a)), instead of $g^{(2)}(0) = 1$ for a coherent pump. This intensity fluctuation is further amplified by the non-linear SFWM process, leading to a stronger bunching of $g^{(2)}(0) = 2.551$ measured in the unheralded C28 SFWM output. As a result, the heralded $g_h^{(2)}(0)$ values become considerably worse than the coherent pump limit, see experimental data (blue dots) in Fig. 1 (b). The measured data are in good agreement with the theoretical prediction (dashed line) using an unheralded $g^{(2)}(0)$ value of 2.551. The general expression of $g_h^{(2)}(0)$ for an arbitrary photon number distribution is given in Eq. (A6) in Appendix A.

As summarised in Fig. 1 (b), previous HSPS sources have $g_h^{(2)}(0)$ values that are worse than the theoretical limit although impressive $g_h^{(2)}(0)$ and CAR values were obtained [11–15]. To further appreciate the advance our HSPS brings, we list the state-of-the-art SFWM photon pair sources under pulsed excitation in Table I. Our device is advantageous over all parameter spaces, including repetition rate, CAR, and $g_h^{(2)}(0)$.

V. CONCLUSION

We have derived a theoretical limit for single-photon purity of an HSPS under coherent pump condition, and subsequently verify it on an on-chip SFWM source based on SOI platform. The source exhibits an unprecedented coincidence counting rate of 1.51 MHz together with a measured CAR of 16.77. Moreover, we measure an ultra low $g_h^{(2)}(0)$ value of 0.00094 ± 0.00002 . Thanks to its

pulsed operation, we expect our high-quality HSPS to be useful in quantum information applications.

Note added. During the revision of the present work, we became aware of a recent work demonstrating a low loss, highly stable and re-useable edge coupler for high heralding efficiency and having claimed a low $g_h^{(2)}(0)$ value of 0.0004 [22]. However, the reported $g_h^{(2)}(0)$ value has a vast uncertainty and still deviates from the theoretical limit.

ACKNOWLEDGEMENTS

This work is supported by National Natural Science Foundation of China under Grants 12105010 (Q. Z.), 62105034 (L. Z.), and 62250710162 (Z. Y.).

Appendix A: Theoretical analysis of second-order correlation functions $g_h^{(2)}(0)$

For a heralded single photon source (HSPS), the heralded second-order correlation function is shown as Eq. (1). As measurements between the heralding side and the heralded are independent, operators \hat{a}_1 and $\hat{a}_{2,3}$ are commutative. Therefore, $g_h^{(2)}(0)$ can be rewritten as

$$g_h^{(2)}(0) = \frac{\langle \hat{n}_s \hat{n}_i (\hat{n}_i - 1) \rangle}{\langle \hat{n}_s \hat{n}_i \rangle^2} \langle \hat{n}_s \rangle, \quad (\text{A1})$$

where \hat{n} represents the photon number operator, the angle brackets represent the expected value, and the subscripts s and i refer to the signal photons used for heralding and the idler photons being heralded, respectively.

Due to the simultaneity of photon pairs generated through SFWM, the photon pair state can be written as [5]

$$|\Phi\rangle = \sum_{n=0}^{\infty} P(n) |n, n\rangle_{s,i}, \quad (\text{A2})$$

where $P(n)$ is the probability of generating n photon pairs per pulse.

Then, we can calculate the second-order correlation function of the heralded single-photon source $g_h^{(2)}(0)$ under any distribution by taking Eq. (A2) into Eq. (A1), it can be written as

$$\begin{aligned} g_h^{(2)}(0) &= \frac{\langle \Phi | \hat{n}_s \hat{n}_i (\hat{n}_i - 1) | \Phi \rangle}{\langle \Phi | \hat{n}_s \hat{n}_i | \Phi \rangle^2} \langle \Phi | \hat{n}_s | \Phi \rangle \\ &= \frac{\sum n^2(n-1)P(n)}{(\sum n^2 P(n))^2} \sum n P(n). \end{aligned} \quad (\text{A3})$$

Therefore, for SFWM sources with Poissonian distribution, $P(n) = e^{-\mu} \frac{\mu^n}{n!}$, its $g_h^{(2)}(0)$ can be expressed as.

$$g_h^{(2)}(0) = \frac{\mu^2(\mu + 2)}{[\mu(\mu + 1)]^2} \mu = 1 - \frac{1}{(\mu + 1)^2}. \quad (\text{A4})$$

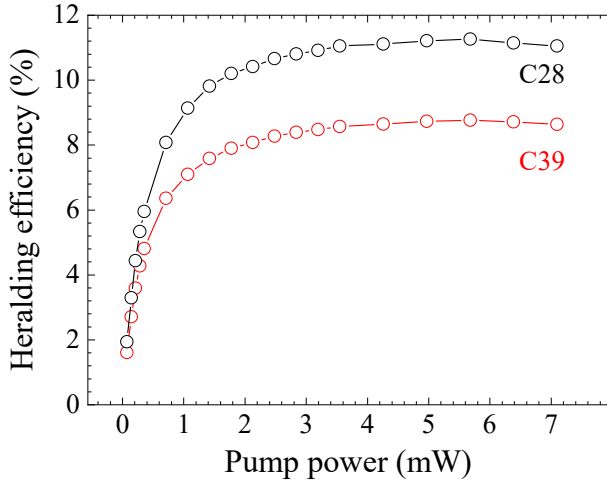


FIG. 6. Results of heralding efficiencies.

When intensity fluctuation exists, it can be assumed that the photon number distribution is given as a statistical mixture of Poissonian distributions with different values of mean photon number [19],

$$P(n) = \int d\mu f(\mu) e^{-\mu} \frac{\mu^n}{n!}. \quad (\text{A5})$$

With this distribution, one can obtain $g_h^{(2)}(0)$ at arbitrary photon number distributions

$$g_h^{(2)}(0) = \frac{\langle \mu^3 \rangle + 2\langle \mu^2 \rangle}{(\langle \mu^2 \rangle + \langle \mu \rangle)^2} \langle \mu \rangle = \frac{g^{(3)}(0)\bar{\mu}^2 + 2g^{(2)}(0)\bar{\mu}}{(g^{(2)}(0)\bar{\mu} + 1)^2}, \quad (\text{A6})$$

where $\bar{\mu}$ refers to the expectation value of μ with distribution function $f(\mu)$, $g^{(2)}(0)$ and $g^{(3)}(0)$ is the second order correlation function and third order correlation function of HSPS under unheraled conditions, respectively. When $\bar{\mu} \ll 1$, Eq. (A6) can be approximated as $\frac{2g^{(2)}(0)\bar{\mu}}{(g^{(2)}(0)\bar{\mu} + 1)^2}$. Therefore, we can measure $g^{(2)}(0)$ under unheraled con-

ditions to evaluate the impact of pump light intensity fluctuation on the single-photon purity of HSPS.

Appendix B: Heralding efficiency

As the photons are generated in pairs, one defines the probability of obtaining a heralding event by detecting the other photon as *heralding efficiency*, which can be expressed as $\eta_{h_{s(i)}} = \frac{C}{S_{i(s)}}$ [23]. Ideally, heralding efficiency is equivalent to the collection efficiency of the signal (idler) photons.

From Fig. 6, we can see that as the pump power increases, the heralding efficiency continues to increase and then approaches saturation. This is because when the incident pump power is low, the noise photons account for the majority. As the power increases, due to the quadratic dependence of the generated photons on power and the linear dependence of noise photons on power, photons generated by SFWM gradually dominate the single counting. At the point that the SFWM reaches saturation—mostly caused by the two-photon absorption effect in silicon, the heralding efficiency reaches saturation as well. We measured a maximum heralding efficiency of 11.3% at the pump power of 5.68 mW in channel C28. However, a significant gap of approximately 1 dB between the heralding efficiency and theoretical values, i.e., the channel loss, is observed. This gap is mainly caused by the narrow-band filtering of DWDM, which leads to part of the signal and idler photons do not contribute to the coincidence counts [24].

Appendix C: Coincidence to accidental ratio (CAR)

Figure 7(a) shows an example correlation histogram, which was measured between C28 and C39 DWDM channels under an on-chip power of 0.35 mW. In extracting the CAR value, we choose a time-bin width of $\tau = 0.4$ ns to cover the entire coincidence peak. The measured CAR versus coincidence counting rate is shown in Fig. 7(b). We measured a CAR of approximately 17 at a maximum coincidence counting rate of 1.51 MHz. At an on-chip pump average power of 0.07 mW, we measured a maximum CAR of 4630.

[1] C. Couteau, S. Barz, T. Durt, T. Gerrits, J. Huwer, R. Prevedel, J. Rarity, A. Shields, and G. Weihs, Applications of single photons to quantum communication and computing, *Nat. Rev. Phys.* **5**, 326 (2023).

[2] Y. Yu, S. Liu, C.-M. Lee, P. Michler, S. Reitzenstein, K. Srinivasan, E. Waks, and J. Liu, Telecom-band quantum dot technologies for long-distance quantum networks, *Nat. Nanotechnol.* **18**, 1389 (2023).

[3] P. G. Kwiat, E. Waks, A. G. White, I. Appelbaum, and P. H. Eberhard, Ultrabright source of polarization-entangled photons, *Phys. Rev. A* **60**, R773 (1999).

[4] J. Chen, X. Li, and P. Kumar, Two-photon-state generation via four-wave mixing in optical fibers, *Phys. Rev. A* **72**, 033801 (2005).

[5] S. Signorini and L. Pavesi, On-chip heralded single photon sources, *AVS Quantum Sci.* **2**, 041701 (2020).

[6] H. Wang, Q. Zeng, H. Ma, and Z. Yuan, Progress on chip-based spontaneous four-wave mixing quantum light sources, *Adv. Dev. Instrum.* **5**, 0032 (2024).

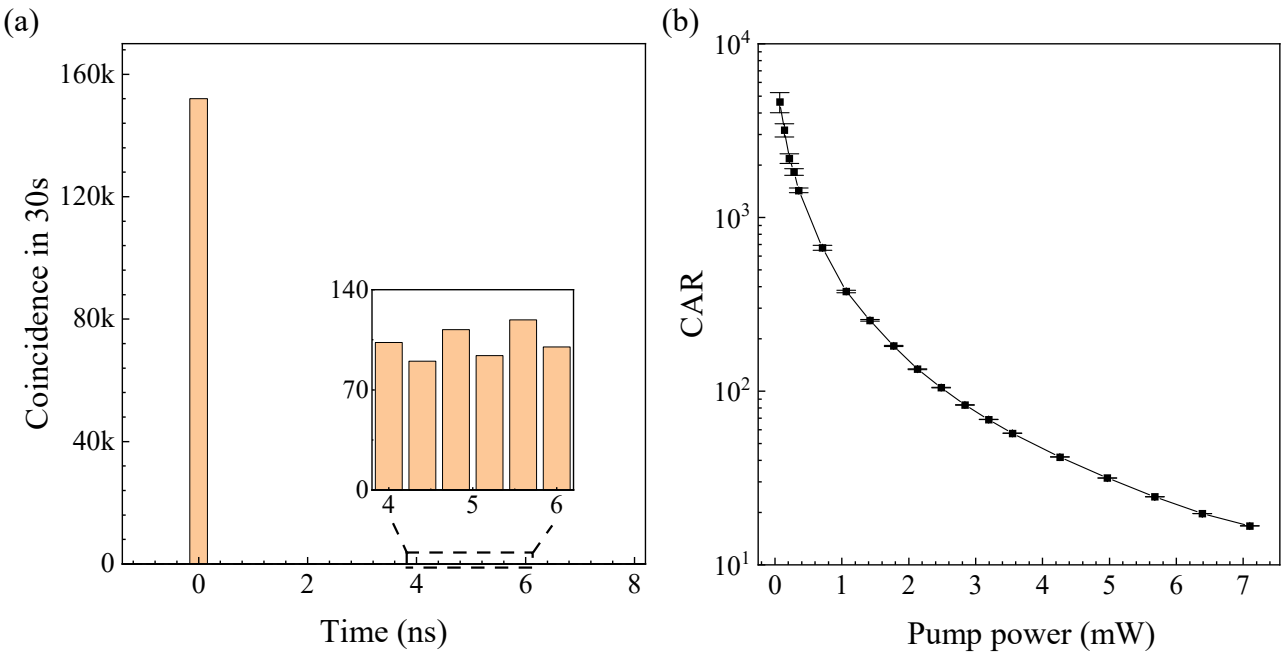


FIG. 7. (a) Coincidence histogram measured with 30 s integration time and at a pump power of 0.35 mW. Inset: magnified view of a section of the accidental coincidences. (b) CAR versus pump power.

- [7] Z. L. Yuan, B. Fröhlich, M. Lucamarini, G. L. Roberts, J. F. Dynes, and A. J. Shields, Directly Phase-Modulated Light Source, *Phys. Rev. X* **6**, 031044 (2016).
- [8] Q. Zeng, H. Wang, H. Yuan, Y. Fan, L. Zhou, Y. Gao, H. Ma, and Z. Yuan, Controlled Entanglement Source for Quantum Cryptography, *Phys. Rev. Appl.* **19**, 054048 (2023).
- [9] H. Takesue and K. Shimizu, Effects of multiple pairs on visibility measurements of entangled photons generated by spontaneous parametric processes, *Opt. Commun.* **283**, 276 (2010).
- [10] M. Collins, C. Xiong, I. Rey, T. Vo, J. He, S. Shahnia, C. Reardon, T. Krauss, M. Steel, A. Clark, and B. Eggleton, Integrated spatial multiplexing of heralded single-photon sources, *Nat. Commun.* **4**, 2582 (2013).
- [11] K. Guo, E. N. Christensen, J. B. Christensen, J. G. Koe foed, D. Bacco, Y. Ding, H. Ou, and K. Rottwitt, High coincidence-to-accidental ratio continuous-wave photon-pair generation in a grating-coupled silicon strip waveguide, *Appl. Phys. Express* **10**, 062801 (2017).
- [12] C. Xiong, M. J. Collins, M. J. Steel, T. F. Krauss, B. J. Eggleton, and A. S. Clark, Photonic Crystal Waveguide Sources of Photons for Quantum Communication Applications, *IEEE J. Sel. Top. Quantum Electron.* **21**, 205 (2015).
- [13] C. Ma, X. Wang, V. Anant, A. D. Beyer, M. D. Shaw, and S. Mookherjea, Silicon photonic entangled photon-pair and heralded single photon generation with $CAR > 12,000$ and $g^{(2)}(0) < 0.006$, *Opt. Express* **25**, 32995 (2017).
- [14] T. J. Steiner, J. E. Castro, L. Chang, Q. Dang, W. Xie, J. Norman, J. E. Bowers, and G. Moody, Ultrabright Entangled-Photon-Pair Generation from an AlGaAs-On-Insulator Microring Resonator, *PRX Quantum* **2**, 010337 (2021).
- [15] M. Jin, N. MacFarlane, Z. Ma, Y. M. Sua, M. Foster, Y. Huang, and A. Foster, Photon-Pair Generation in a Heterogeneous Nanophotonic Chip, *ACS Photonics* **10**, 1962 (2023).
- [16] L. C. Comandar, M. Lucamarini, B. Fröhlich, J. F. Dynes, Z. L. Yuan, and A. J. Shields, Near perfect mode overlap between independently seeded, gain-switched lasers, *Opt. Express* **24**, 17849 (2016).
- [17] J. Monteleone, III, M. van Niekerk, M. Ciminelli, G. Leake, D. Coleman, M. Fanto, and S. Preble, Packaged foundry-fabricated silicon spiral photon pair source, in *QUANTUM NANOPHOTONIC MATERIALS, DEVICES, AND SYSTEMS 2022*, Proceedings of SPIE, Vol. 12206, edited by C. Soci, M. Sheldon, M. Agio, and I. Aharonovich (SPIE, 2022) conference on Quantum Nanophotonic Materials, Devices, and Systems Part of SPIE Nanoscience and Engineering Conference, San Diego, CA, AUG 21-25, 2022.
- [18] J. F. Dynes, M. Lucamarini, K. A. Patel, A. W. Sharpe, M. B. Ward, Z. L. Yuan, and A. J. Shields, Testing the photon-number statistics of a quantum key distribution light source, *Opt. Express* **26**, 22733 (2018).
- [19] K. Nakata, A. Tomita, M. Fujiwara, K.-i. Yoshino, A. Tajima, A. Okamoto, and K. Ogawa, Intensity fluctuation of a gain-switched semiconductor laser for quantum key distribution systems, *Opt. Express* **25**, 622 (2017).
- [20] C. Xiang, W. Jin, J. Guo, C. Williams, A. M. Netherton, L. Chang, P. A. Morton, and J. E. Bowers, Effects of nonlinear loss in high-Q Si ring resonators for narrow-linewidth III-V/Si heterogeneously integrated tunable lasers, *Opt. Express* **28**, 19926 (2020).
- [21] M. Bock, A. Lenhard, C. Chunnillall, and C. Becher, Highly efficient heralded single-photon source for telecom wavelengths based on a ppls waveguide, *Opt. Express* **24**, 23992 (2016).

- [22] J. Du, G. F. R. Chen, H. Gao, J. A. Grieve, D. T. H. Tan, and A. Ling, Demonstration of a low loss, highly stable and re-useable edge coupler for high heralding efficiency and low $g(2)(0)$ SOI correlated photon pair sources, *Opt. Express* **32**, 11406 (2024).
- [23] D. N. Klyshko, Use of two-photon light for absolute calibration of photoelectric detectors, *Sov. J. Quantum Electron.* **10**, 1112 (1980).
- [24] E. Meyer-Scott, N. Montaut, J. Tiedau, L. Sansoni, H. Herrmann, T. J. Bartley, and C. Silberhorn, Limits on the heralding efficiencies and spectral purities of spectrally filtered single photons from photon-pair sources, *Phys. Rev. A* **95**, 061803 (2017).